

Electrostatic Influence of Local Cysteine Environments on Disulfide Exchange Kinetics[†]

Grayson H. Snyder,* Michael J. Cennerazzo, Anthony J. Karalis, and Dorothy Field

ABSTRACT: The ionic strength dependence of the bimolecular rate constant for reaction of the negative disulfide 5,5'-dithiobis(2-nitrobenzoic acid) with cysteines in fragments of naturally occurring proteins was determined by stopped-flow spectroscopy. The Debye-Hückel relationship was applied to determine the effective charge at the cysteine and thereby determine the extent to which nearby neighbors in the primary sequence influence the kinetics. Corrections for the secondary salt effect on cysteine pKs were determined by direct spectrometric pH titration of sulfhydryl groups or by observation of the ionic strength dependence of kinetics of cysteine reaction with the neutral disulfide 2,2'-dithiodipyridine. Quantitative expressions were verified by model studies with *N*-acetylcysteine. At ionic strengths equal to or greater than 20 mM, the net charge at the polypeptide cysteine site is the sum of the single negative charge of the thiolate anion and the charges

of the amino acids immediately preceding and following the cysteine in the primary sequence. At lower ionic strengths, more distant residues influence kinetics. At pH 7.0, 23 °C, and an ionic strength of 20 mM, rate constants for reaction of the negative disulfide with a cysteine having two positive neighbors, one positive and one neutral neighbor, or two neutral neighbors are 132 000, 3350, and 367 s⁻¹ M⁻¹, respectively. This corresponds to a contribution to the activation energy of 0.65–1.1 kcal/mol per ion pair involved in collision between the cysteine and disulfide regions. The results permit the estimation that cysteine local environments may provide a means of achieving a 10⁶-fold range in rate constants in disulfide exchange reactions in random-coil proteins. This range may prove useful in developing strategies for directing disulfide pairing in synthetic proteins.

Attempts to design functional proteins with nonnatural sequences have focused on two classes of molecules, small cyclic peptides which bind ions and may function in membrane transport (Davis et al., 1976) and lysine- or arginine-containing peptides which inhibit trypsin (Tan & Kaiser, 1976; Weber & Schmid, 1976). The medicinal interest in trypsin inhibitors derives from the numerous examples of trypsinlike enzymes and their inhibitors in physiological processes (Perutz, 1976). Examples include digestion, blood clotting, complement fixation, ovum fertilization, and cell-surface interactions. Trypsin inhibitors are one example of a large variety of natural enzyme inhibitors whose structures consist of a small disulfide-cross-linked polypeptide main frame with a protruding amino acid similar in character to the enzyme's natural substrate. Examples include the positive lysine-15 protruding from bovine pancreatic trypsin inhibitor (Ruhlmann et al., 1973), the nonpolar leucine-53 in the chymotrypsin inhibitor from lima beans (Stevens et al., 1973), the negative backbone terminal carboxyl group in potato carboxypeptidase inhibitor (Hass et al., 1976), and lysine-47 in cobrotoxin (Chang et al., 1971).

The lysine side chain in the latter example mimics acetylcholine, enabling the snake venom toxin to inhibit the acetylcholine receptor. Sequences of at least seven unrelated families of trypsin inhibitors are known (Dayhoff, 1978). These families have different primary structures, suggesting that several natural geometries satisfy requirements for trypsin inhibition. This promotes the hope that additional man-made geometries could exist.

In the absence of a complete knowledge of how a protein's primary sequence directs folding to the native tertiary structure, no general strategies exist for designing a primary sequence whose chemical synthesis would give a protein with a desired topology. Many attempts to construct enzyme inhibitors, therefore, consist of synthesizing peptides whose sequences resemble portions of native inhibitors. If strategies could be developed to direct formation of a specific set of disulfide bridges in a synthetic polypeptide chain with four or more cysteines, it might be possible to achieve formation of disulfide-cross-linked main frames with specific topologies. Active enzyme inhibitors then might be constructed by adding appropriate residues to the sequence to give a protruding active amino acid on the main-frame's surface.

Strategies for directing disulfide pairing would need to consider factors such as the relative positioning of cysteines in the sequence, the presence of aromatic or electrostatically charged neighbors in cysteine local environments, and the overall redox potential of the solution. Cysteines separated

[†] From the Department of Biological Sciences, State University of New York, Buffalo, New York 14260. Received May 27, 1981. Supported by Grant GM 26715 from the National Institutes of Health, Biomedical Research Support Grant funds from the National Institutes of Health to the State University of New York at Buffalo, and the University Awards Committee of the Research Foundation of the State University of New York.

by less than four residues in the primary sequence are unlikely to pair with each other to form an intramolecular disulfide-bridged loop due to steric constraints imposed in a small ring (Hardy et al., 1971). For larger separations, random intramolecular collisions between cysteines are possible, with the probability of collision decreasing as the separation in the sequence increases (Kauzmann, 1959). Aromatic neighbors may stabilize disulfides by forming S- π complexes (Morgan et al., 1978; Bodner et al., 1980). Neighboring histidines may enhance a cysteine's participation in disulfide exchange reactions (Wenck & Schneider, 1971). Charged amino acids may electrostatically influence the pKs and reactivities of neighboring cysteines and the frequency of collisions between cysteine and disulfide regions. In a strongly oxidizing medium, topologies with cysteines in a position to give complete disulfide pairing would be favored over structures with two or more reduced cysteines.

This paper considers electrostatic influences of local cysteine environments on the kinetics of disulfide exchange reactions. The first objective is to determine whether the polypeptide residues which are adjacent to a cysteine in the primary sequence can exert a significant effect on disulfide exchange. If so, the second objective is to estimate the order of magnitude of the possible range in values of rate constants which may be achieved by altering the charge of a cysteine's immediate neighbors.

Electrostatic effects are exhibited in disulfide exchange reactions between small organic molecules (Hird, 1962; Sza-jewski & Whitesides, 1980). For example, under particular conditions, negative dithiothreitol attacks the disulfide of positive cystamine more than 100 times as fast as it attacks the disulfide of negative dithiodiglycolic acid (Creighton, 1975). In these molecules, the charged groups are separated from the sulfurs by two or three bonds, such that the charged groups exert their effect both by Coulombic forces acting through space and by inductive effects through the bonds which alter the electron density on the sulfur atoms. In proteins, a minimum of seven bonds separate the charged group and the sulfur (seven bonds for an aspartate-cysteine or cysteine-aspartate sequence) such that only Coulombic forces are available. Very little published data exist for such systems. In one study on small peptides, intramolecularly oxidized cysteine-lysine(+)-cysteine methyl ester is attacked twice as fast by negative glutathione S⁻ as oxidized cysteine-glutamate(-)-cysteine methyl ester at pH 7, 25 °C, and a high ionic strength of 0.7 M (Weber & Hartter, 1974). The experiments in this paper investigate the ionic strength dependence of the reaction of the negative disulfide 5,5'-dithiobis(2-nitrobenzoic acid) (DTNB)¹ and the neutral disulfide DTP with cysteine derivatives and cyanogen bromide fragments of commercially available proteins. Use of the Debye-Hückel relationship, modified to include secondary salt effects on the sulfhydryl pK_a of the cysteines, permits determination of the effective charge at cysteines having different local ionic environments. This provides a means of distinguishing between contributions from amino acids immediately adjacent to the cysteine and residues two or more positions away in the sequence. Comparison of the absolute values of rate constants permits estimation of the range of achievable

electrostatic effects.

Experimental Procedures

Materials. Kunitz soybean trypsin inhibitor, hen egg white lysozyme, porcine pepsin, DTNB, DTP, Ac-Cys, monothio-glycerol, and dansylated amino acids were purchased from Sigma Chemical Co. Cys-OEt and valine-isoleucine were obtained from Vega Biochemicals. Amino acid derivatives and disulfide reagents were used without further purification. Sephadex gel filtration and ion-exchange resins were obtained from Pharmacia Fine Chemicals. Chen-Chin polyamide sheets were purchased from Gallard-Schlesinger.

Purification of Reduced Two-Cysteine Fragments. Soybean trypsin inhibitor was purified by ion-exchange chromatography on DEAE-cellulose (Bieth & Frechin, 1974). CNBr fragments with intact disulfides were separated by Sephadex G100 gel filtration to give the pure fragment STI (Koide & Ikenaka, 1973). After lysozyme was cleaved with CNBr and the disulfides in the product were reduced, reduced fragments were separated by Sephadex G25 gel filtration to obtain purified LYS (Archarya & Taniuchi, 1976). CNBr fragments of pepsin with disulfides intact were separated by Sephadex G75 gel filtration and ion-exchange chromatography by using previously published column conditions (Chen et al., 1975). The identities of isolated peaks were determined by amino acid analysis on a Beckman 121 MB analyzer and by dansyl end-group determinations on polyamide sheets (Lee & Saffile, 1976). Peptide disulfides were reduced with dithiothreitol at pH 8.7 for 30 min at 40 °C. Reduced peptides were stored at 4 °C under N₂ in 1 mM HCl, conditions where STI and LYS are soluble but PEP is precipitated. Concentrations of free SH were determined by spectrophotometric titration with excess DTNB, using TNB $\epsilon_{412} = 14\,150\text{ M}^{-1}\text{ cm}^{-1}$ at pH 7.3 and 25 °C (Riddles et al., 1979). ϵ_{280} for PEP was determined directly by quantitative amino acid analysis using norleucine as an internal standard. ϵ_{280} values for LYS and STI were estimated by using ϵ_{280} tyrosine = $1197\text{ M}^{-1}\text{ cm}^{-1}$ and ϵ_{280} tryptophan = $5559\text{ M}^{-1}\text{ cm}^{-1}$ at pH 7.0 (Mihalyi, 1969). All three fragments had 1.8–2.2 SH groups/peptide when assayed by these procedures.

Calibration of the Stopped-Flow Spectrophotometer. A stopped-flow spectrophotometer was assembled from commercially available components, including a Spex 0.22-m double-grating monochromator, a thermostated Aminco-Morrow stopped-flow assembly, and a Nicolet Explorer transient recorder. Wavelengths were calibrated with a holmium oxide filter obtained from Gilford. Slits and lamp intensities were adjusted to prevent photomultiplier saturation and ensure that output voltages were proportional to transmittance, using calibrated solutions of 2-thiopyridone and acidified bromophenol blue at 343 and 412 nm, respectively, wavelengths where DTP and DTNB kinetics were analyzed. Time intervals between triggering of the transient recorder, mixing of the reagents, and stopping of the flow were calibrated by the biphasic disulfide exchange reaction between excess thioglycerol and DTNB (Paul et al., 1980). Overall instrument performance and data reduction procedures were monitored by reproducing previously published results for the rate of decarboxylation of carbonic acid (Berger & Stoddart, 1965), monitoring OD changes in the pH indicator bromophenol blue.

Stopped-Flow Reactions and pK Determinations. Stopped-flow kinetics for reactions of LYS and STI were performed by mixing a solution of peptide in 1 mM HCl with a buffered solution of DTNB or DTP containing 10 mM imidazole and varying NaCl concentrations. Because PEP is insoluble at pH

¹ Abbreviations used: DTNB, 5,5'-dithiobis(2-nitrobenzoic acid); TNB, 5-thio-2-nitrobenzoic acid; DTP, 2,2'-dithiodipyridine; EDTA, ethylenediaminetetraacetic acid; Ac-Cys, N-acetyl-L-cysteine; Cys-OEt, L-cysteine ethyl ester; STI, Kunitz soybean trypsin inhibitor fragment 115–181; LYS, hen egg white lysozyme fragment 106–129; PEP, porcine pepsin fragment 290–333; CNBr, cyanogen bromide; Cys, cysteine.

3 but readily redissolves at pH 7, stock suspensions of PEP were diluted into freshly degassed imidazole buffers at pH 7 immediately before use in the spectrometer. Concentrations of stock solutions of DTP and DTNB were determined spectrophotometrically by using $\epsilon_{281} = 9730 \text{ M}^{-1} \text{ cm}^{-1}$ at pH 7.2 (Grassetti & Murray, 1967) and $\epsilon_{324} = 17780 \text{ M}^{-1} \text{ cm}^{-1}$ at pH 7.3 and 25°C (Riddles et al., 1979), respectively. The ΔOD values obtained in the spectrometer in kinetic studies corresponded to expected values for stoichiometric generation of 2-thiopyridone ($\epsilon_{343} = 7060 \text{ M}^{-1} \text{ cm}^{-1}$ at pH 7.2; Grassetti & Murray, 1967) and 5-thio-2-nitrobenzoic acid ($\epsilon_{412} = 14150 \text{ M}^{-1} \text{ cm}^{-1}$ at pH 7.3, 25°C ; Riddles et al., 1979), such that it is unlikely that kinetics correspond to reactions with minor impurities in the DTNB or DTP. The pHs of the reaction mixtures were measured immediately after acquiring kinetic data. Ionic strengths at low NaCl concentrations were calculated by using an imidazole $pK = 6.99$ (Datta & Grzybowski, 1966) obtained at 25°C and μ (ionic strength) = 0 M. Changes in this pK at high ionic strengths will not significantly alter the calculations since imidazole makes a minor contribution relative to NaCl under those conditions.

Complete UV spectra of Ac-Cys in the SH form (low pH) and S^- form (high pH) were obtained on an Aminco-Chance DW-II spectrometer and revealed that the wavelength of greatest difference in absorption equals 239 nm. Aliquots of stock solutions of Ac-Cys in 1 mM HCl were diluted into degassed buffers of different pH and ionic strength, and the OD_{239} was measured immediately. pHs were measured with a Radiometer PHM26 pH meter equipped with a GK2421C electrode. KCl was used to give high ionic strengths to minimize Na^+ effects on the glass electrode. At each ionic strength, ten or more samples were prepared which ranged from pH 6.8 to 11.8. At low salt concentrations, ionic strengths were calculated by using the imidazole pK referred to above, pK orthoboric acid = 9.24 (Owen, 1934), and pK piperidine = 11.12 (Bates & Bower, 1956) obtained at 25°C , $\mu = 0 \text{ M}$. Data from spectrophotometric titrations of Ac-Cys were fit to the following expression to obtain pK_s :

$\text{OD}_{239} =$

$$L[\text{Ac-Cys}]_{\text{total}} \left[\epsilon_{\text{S}^-} + (\epsilon_{\text{SH}} - \epsilon_{\text{S}^-}) \left(\frac{10^{\text{pH}-\text{pK}}}{1 + 10^{\text{pH}-\text{pK}}} \right) \right] \quad (1)$$

where L = optical cell path length.

Results

Purification of PEP. Previously published column conditions for purifying CNBr-cleaved pepsin with disulfides reduced and cysteines aminoethylated (Chen et al., 1975) were employed here for purifying fragments with disulfides intact. The G75 profile looked similar to the published results for aminoethylated derivatives, and the fifth peak was purified on DEAE-Sephadex. It elutes at 0.48 M NaCl instead of at the 0.40 M NaCl position obtained with the less negative aminoethylated derivative but still corresponds to fragment 290–333. The identity of PEP was confirmed by amino acid analysis. Furthermore, dansyl end-group determinations indicated N-terminal valine or valine-isoleucine as expected.

Ionic Strength Dependence of the Sulfhydryl pK_a of Ac-Cys. The sulfhydryl pK_s were obtained by previously published procedures (Benesch & Benesch, 1955) at four different ionic strengths and are given in Figure 1. The ionic strength dependence of the pK_s was fit to the following relationship [based on Neuberger (1937)]²

$$pK = pK^0 + (Z_{\text{acid}}^2 - Z_{\text{base}}^2) \frac{A\mu^{1/2}}{1 + Br_1\mu^{1/2}} \quad (2)$$

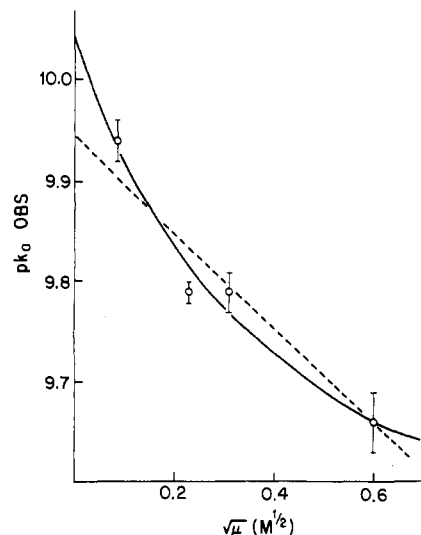


FIGURE 1: Ionic strength dependence of the sulfhydryl pK_a of *N*-acetylcysteine. Conditions were as follows: 35.7 μM Ac-Cys, 9 mM orthoboric acid, 9 mM imidazole, 9 mM piperidine, and KCl adjusted to give indicated $\mu^{1/2}$; $T = 23^\circ \text{C}$. $Z_{\text{acid}}^2 - Z_{\text{base}}^2 = -3$ (solid line) or -1 (dashed line).

where Z indicates the ionic charge of the protonated acid species or deprotonated base species, r is related to the distance of closest approach between reactant species and counterions, and A and B have values of $0.509 \text{ M}^{-1/2}$ and $3.29 \text{ M}^{-1/2} \text{ nm}^{-1}$, respectively [e.g., see Nolte et al. (1980)] in aqueous solution at 25°C . The solid line in Figure 1 includes the charge of the carboxyl group in the calculations, giving $Z_{\text{acid}} = -1$ and $Z_{\text{base}} = -2$. This fit gives $pK^0 = 10.04 \pm 0.02$ and $r_1 = 0.72 \pm 0.12 \text{ nm}$. The dashed line in Figure 1 neglects the carboxyl group such that $Z_{\text{acid SH}} = 0$ and $Z_{\text{base S}^-} = -1$. For this fit, $r_1 = 0.03 \pm 0.10 \text{ nm}$, an unreasonable value. The former fit was used to calculate the fraction of Ac-Cys molecules in the thiolate form, using eq 2 and

$$f_{\text{S}^-} = \frac{10^{\text{pH}-\text{pK}}}{1 + 10^{\text{pH}-\text{pK}}} \quad (3)$$

At pH 7.0, the calculated f_{S^-} increases 2.8-fold from 9.13×10^{-4} to 2.59×10^{-3} as μ increases from 0 to 1.0 M.

Kinetics of Reaction of Ac-Cys with DTNB. The disulfide exchange reaction between Ac-Cys and DTNB includes the following possible steps:

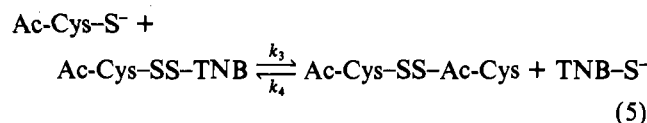
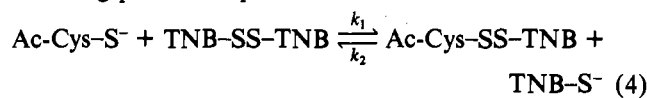


Figure 2 presents the biphasic kinetics resulting from reaction of an excess of Ac-Cys with DTNB, monitoring formation of TNB-S^- at 412 nm. After the transient was accumulated, data were plotted on an X-Y recorder, digitized, and analyzed on a Wang computer by nonlinear least-squares analysis. Raw data obtained as millivolt output from the photomultiplier were converted to OD values with

$$\text{OD}_t = \log \left(\frac{\text{mV}_{100\% \text{ transmittance}} - \text{mV}_{0\% \text{ transmittance}}}{\text{mV}_t - \text{mV}_{0\% \text{ transmittance}}} \right) \quad (6)$$

² In all equations, the superscript 0 indicates zero ionic strength, the superscript ∞ indicates infinite ionic strength, and the subscript 0 indicates time zero, the initial moment of mixing of solutions in the stopped-flow spectrometer.

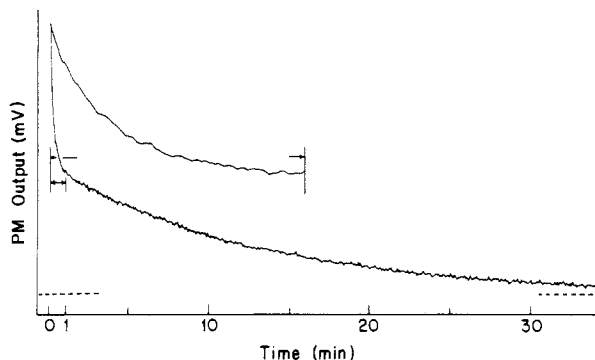


FIGURE 2: Reaction of DTNB with excess acetylcysteine. Conditions were as follows: 0.577 mM Ac-Cys, 5.15 μ M DTNB, 9.50 mM imidazole, 29.6 mM NaCl, and 2.49 mM EDTA, pH 6.95; μ = 44.9 mM; T = 22.9 $^{\circ}$ C. Abscissa scale = lower trace; upper trace = 16 \times horizontal expansion of first minute. Dashed line = final millivolts at equilibrium.

The calculated OD values were fit to the sum of two exponentials:

$$\Delta OD_t = \Delta OD_0 [\text{amp}_I e^{-k_{I, \text{obs}} t} + (1 - \text{amp}_I) e^{-k_{II, \text{obs}} t}] \quad (7)$$

where $\Delta OD_t = OD_t - OD_{\text{equilibrium}}$ and t is the elapsed time since mixing. The amplitudes of both phases are equal ($\text{amp}_I = 0.5$), and each phase gives a change in OD corresponding to 1.0 TNB produced per starting DTNB molecule. Later discussion will suggest that steps 2 and 4 in eq 4 and 5 are insignificant, and the fast and slow steps correspond to steps 1 and 3 in eq 4 and 5, respectively. The relative rates of change in OD differ by a factor of 60, with $k_{\text{obs}, \text{fast}} = (7.48 \pm 0.20) \times 10^{-2} \text{ s}^{-1}$ and $k_{\text{obs}, \text{slow}} = (1.26 \pm 0.05) \times 10^{-3} \text{ s}^{-1}$.

When the same reaction is performed with DTNB concentration in excess over Ac-Cys concentration, the changes in OD give a linear semilogarithmic plot ($\ln |\Delta OD|$ vs. time) corresponding to a single exponential decay with ΔOD resulting from 1.0 TNB produced per starting Ac-Cys and k_{obs} calculated as follows:

$$\Delta OD_t = \Delta OD_0 e^{-k_{\text{obs}} t} \quad (8)$$

Holding $[\text{Ac-Cys}]_0$ constant and varying the value of excess $[\text{DTNB}]_0$, one obtains different values of k_{obs} . A plot of k_{obs} vs. $[\text{DTNB}]_0$ gives a straight line intersecting the origin (data not shown), such that $k_{\text{obs}} = k_1 [\text{DTNB}]_0$ and $k_1 = 132 \pm 5 \text{ s}^{-1} \text{ M}^{-1}$. The discussion below indicates that k_1 corresponds to step 1 in eq 4.

k_1 was determined as a function of ionic strength. Results are given in Figure 3. The fitted line results from application of the following relationship:

$$k = k^0 \times 10^{Z_i Z_j (2A\mu^{1/2}) / (1 + Br_2\mu^{1/2})} (f_S^- / f_S^0) \quad (9)$$

where f_S^- is calculated as described above, Z_i equals the charge of the thiolate form of Ac-Cys, and Z_j equals the charge of DTNB. The terms preceding f_S^- / f_S^0 are the Debye-Hückel relationship for the primary salt effect influencing collision frequencies between simple ions, and the ratio f_S^- / f_S^0 is the secondary salt effect giving the fractional change in the concentration of the reactive species i resulting from changes in the pK . The above function fits the data points well with parameters $k^0 = 20.7 \pm 4.3 \text{ s}^{-1} \text{ M}^{-1}$, $Z_i Z_j = 4.1 \pm 0.8$, and $r_2 = 0.78 \pm 0.14 \text{ nm}$.

Peptides Containing Two Cysteines: Dependence of k_{obs} on $[\text{DTNB}]$. At $\mu = 64 \text{ mM}$ or 1.06 M, the two-cysteine fragment LYS was reacted with an excess of DTNB using varying values of $[\text{DTNB}]_0$. The results are summarized in

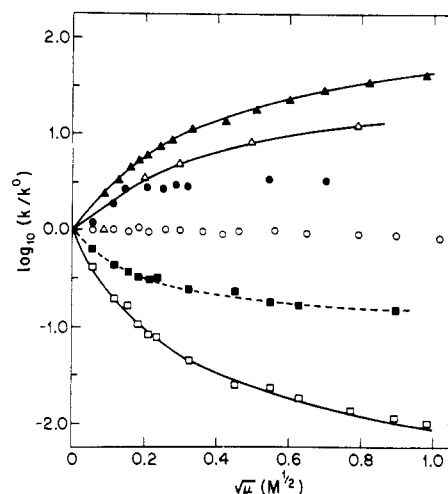


FIGURE 3: Ionic strength dependence of the kinetics of reaction with DTNB and DTP: (\blacktriangle) 20.7 μ M Ac-Cys, 214 μ M DTNB, and 1 mM EDTA, $k^0 = 20.7 \text{ s}^{-1} \text{ M}^{-1}$; (\triangle) 2.93 μ M PEP and 14.4 μ M DTNB, $k^0 = 309 \text{ s}^{-1} \text{ M}^{-1}$; (\bullet) 3.52 μ M STI and 199 μ M DTNB; $k^0 = 1260 \text{ s}^{-1} \text{ M}^{-1}$; (\circ) 20 μ M Cys-OEt and 214 μ M DTNB, $k^0 = 8960 \text{ s}^{-1} \text{ M}^{-1}$; (\square) 0.55 μ M LYS and 22 μ M DTNB, $k^0 = 856000 \text{ s}^{-1} \text{ M}^{-1}$; (\blacksquare) 3.85 μ M LYS and 154 μ M DTP, $k^0 = 22270 \text{ s}^{-1} \text{ M}^{-1}$. All data were measured under the following conditions: 5 mM imidazole; $[\text{NaCl}]$ varied to give indicated $\mu^{1/2}$; $T = 23\text{--}24 \text{ }^{\circ}\text{C}$; pH 6.9–7.0.

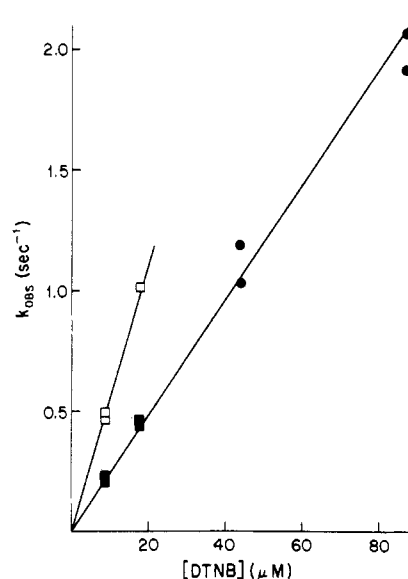
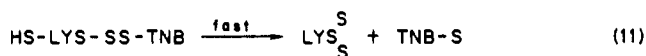
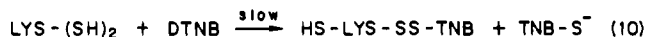
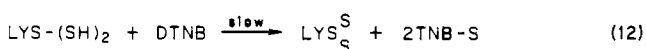


FIGURE 4: Concentration dependence of the kinetics of reaction of LYS with DTNB. Conditions were as follows: 2.17 μ M peptide, 25 mM phosphate, 0.5 mM EDTA, and NaCl added to give $\mu = 64 \text{ mM}$ (\square) or 1.059 M (\blacksquare , \bullet), pH 7.2, $t = 23 \text{ }^{\circ}\text{C}$. (\square and \blacksquare) Obtained with eq 13 and 14; (\bullet) single exponential.

Figure 4. For values of $[\text{DTNB}]_0 > 10[\text{SH}]_0$, the observed changes in OD correspond to a single exponential decay and were fit to eq 8. Later discussion will suggest that LYS behaves according to the following mechanism:



which is kinetically equivalent to a single irreversible rate-limiting step



At lower DTNB/peptide ratios, a significant fraction of DTNB would be consumed by reaction with peptide. Under these

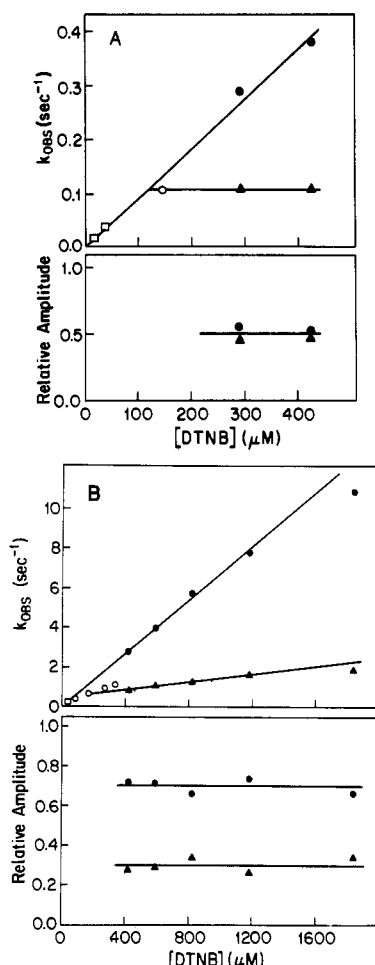


FIGURE 5: Concentration dependence of the kinetics of reaction of PEP and STI with DTNB. (A) PEP (2.93 μM), 5 mM imidazole, and NaCl added to give $\mu = 40$ mM, pH 6.95–7.00, $T = 23$ °C. (□) Obtained with eq 13 and 14; (○) single exponential; (● and ▲) sum of two exponentials, (●) fast phase and (▲) slow phase. (B) STI (3.48 μM), 7.86 mM imidazole, and NaCl added to give $\mu = 40$ mM, $T = 24$ °C, pH 7.1–7.2. Symbols as described in (A).

conditions, data were fit by the following general relationship corresponding to a single bimolecular rate-limiting step

$$\text{OD}_t = \text{OD}_0 + \left\{ \frac{\Delta\epsilon[\text{DTNB}]_0[1 - e^{-(\text{DTNB})_0[\text{peptide}]_0 k_{\text{bimolecular}} t}]}{1 - \left[\frac{[\text{DTNB}]_0}{[\text{peptide}]_0} \right] [1 - e^{-(\text{DTNB})_0[\text{peptide}]_0 k_{\text{bimolecular}} t}]} \right\} \quad (13)$$

where $\Delta\epsilon = \epsilon_{\text{products}} - \epsilon_{\text{reactants}}$. In this case, $\Delta\epsilon_{412}$ corresponds to production of two TNB-S⁻ from one DTNB and one peptide molecule and therefore is equal to 28 100 M⁻¹ cm⁻¹ (Riddles et al., 1979). The k_{obsd} included in Figure 4 for low DTNB/SH ratios equals $k_{\text{obsd,initial}}$ calculated as follows:

$$k_{\text{obsd,initial}} = k_{\text{bimolecular}}/[\text{DTNB}]_0 = \text{s}^{-1} \quad (14)$$

For all LYS experiments, ΔOD corresponds to 1.0 TNB produced per starting cysteine sulfhydryl group. As seen in Figure 4, k_{obsd} is proportional to $[\text{DTNB}]_0$ both at low and at high ionic strengths.

Results for PEP and STI at $\mu = 40$ mM are summarized in Figure 5. At low $[\text{DTNB}]_0$, k_{obsd} is proportional to $[\text{DTNB}]_0$ as in the LYS case, but at high $[\text{DTNB}]_0$, the semi-logarithmic plots are distinctly nonlinear. Data were fit well with application of eq 7, the sum of two exponentials. A detailed consideration of the complex kinetics at high $[\text{DTNB}]_0$

must await isolation and chemical characterization of intermediate and final reaction products. The studies of the ionic strength dependence of k_{obsd} to be considered below were performed under conditions of low $[\text{DTNB}]_0$ where k_{obsd} results from initial rate-limiting bimolecular reaction of DTNB with peptide.

Ionic Strength Dependence of the Protein Fragment Reactions. For the most part, the rate of reaction of Cys-OEt or STI with DTNB is independent of ionic strength. Cys-OEt data were fit to eq 8 for single exponential kinetics. As seen in Figure 3, k_1 exhibits almost no change as μ is increased from 5.5 mM to 1.0 M. STI exhibits an increase in k_1 as the ionic strength increases from 0 to 20 mM ($\mu^{1/2} = 0.14$ M^{1/2}), but k_1 is essentially invariant at higher salt concentrations. STI data cannot be fit by eq 9.

In Ac-Cys, $f_{\text{S}}/f_{\text{S}}^0$ was calculated from experimental measurements of pK. In LYS, this ratio was obtained empirically by reacting the peptide with the neutral disulfide DTP. This approach will be discussed more fully below. The DTP data in Figure 3 were fit by the following relationship:

$$k = k^0(f_{\text{S}}/f_{\text{S}}^0) = k^0 \times 10^{P1\mu^{1/2}/(1+P2\mu^{1/2})} \quad (15)$$

where $P1 = -5.267$ M^{-1/2} and $P2 = 5.352$ M^{-1/2} are empirically obtained parameters capable of giving the dashed line passing through the data points. By use of these values to provide an $f_{\text{S}}/f_{\text{S}}^0$ for fitting DTNB kinetics by eq 9, the solid line in Figure 3 was obtained with $Z_i Z_j = -3.45 \pm 0.65$ and $r_2 = 0.56 \pm 0.23$ nm.

PEP exhibits a continuously increasing k_1 as the ionic strength rises. The fitted line in Figure 3 comes from using eq 9 but eliminating the $f_{\text{S}}/f_{\text{S}}^0$ term and setting r equal to a value of 0.67 nm, the average of fitted values obtained for Ac-Cys and LYS. The fit gives $Z_i Z_j = +3.7 \pm 0.3$. This numerical value will be interpreted later as an upper limit for the absolute magnitude of the true $Z_i Z_j$ of the primary salt effect.

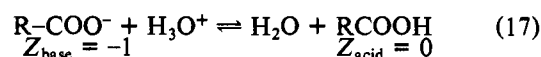
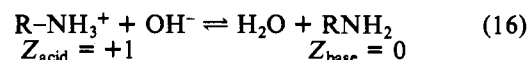
Discussion

Theoretical Background for Consideration of Ac-Cys Data.

The frequency of collisions between charged ions is a function of the sign and magnitude of their charge and the ionic strength of the solution. This primary salt effect is given by eq 9 when $f_{\text{S}}/f_{\text{S}}^0$ equals 1. A summary of many reactions between small ions which exhibit this behavior has been published (LaMer, 1932).

Reactions between ions whose charged groups undergo proton dissociation reactions with water are more complicated. Changes in ionic strength influence not only the frequency of collisions between DTNB (-2) and charged thiol or thiolate regions but also the value of the acid dissociation equilibrium constant (K_a) describing the thiol/thiolate equilibrium. This latter influence is the secondary salt effect.

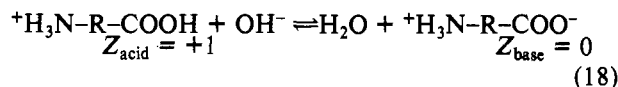
For molecules having a single charged group, the direction and magnitude of the secondary salt effect is known. Data in previous studies (Neuberger, 1937) of the amino group in glycylglycine ester and the carboxyl group in *N*-acetylglutamate were readily fit by eq 2. The two reactions may be represented as follows:



The effect of increased salt concentration is to shift the equilibrium as written to the left, giving a higher $\text{p}K_a$ for

R-NH₃⁺ and a lower pK_a for the carboxyl group.

For molecules with two charged groups separated by a short distance, secondary salt effects are best explained by considering the entire charge of the molecule as a whole, not just the charge of the group whose pK is being studied. In glycylglycine, whose NH₃⁺ and COO⁻ groups are separated by 7 Å (Neuberger, 1937), acid dissociation at the carboxyl group therefore should be written in the form of eq 16 for R-NH₃⁺, not eq 17 for R-COOH:



Thus, at ionic strengths below 20 mM, increased salt concentration shifts the equilibrium as written to the left, giving a higher pK_a for the carboxyl group.

Studies with CPK space-filling models reveal that the COO⁻ and S⁻ groups in Ac-Cys may be separated by a maximum of 5 Å. Similarly in DTNB, a given COO⁻ group may be separated by a maximum of 6 Å from the disulfide. Thus, the above considerations in glycylglycine suggest that the carboxyl groups in Ac-Cys and DTNB will contribute significantly to the kinetics of disulfide exchange between these molecules.

Kinetics of the Reaction of Ac-Cys with DTNB. The reaction of Ac-Cys with DTNB was chosen as a simple system for testing the applicability of quantitative expressions. With Ac-Cys concentration in excess (Figure 2), biphasic behavior is observed. Because the two phases differ by a factor of 60 in velocity, the fast phase corresponds to the approach to an approximate equilibrium for reaction 4, and the slow phase corresponds to the subsequent final approach to equilibrium for the whole system (reactions 4 and 5). Since the ΔOD for the fast phase indicates 1.0 TNB-S⁻ produced per starting DTNB, the first equilibrium lies far to the right in this experiment. With Ac-Cys concentration in excess, [Ac-Cys]_i ≈ [Ac-Cys]₀ = constant such that $k_{\text{obsd,fast}} \approx k_1[\text{Ac-Cys}]_0$, yielding $k_1 = 135 \pm 4 \text{ s}^{-1} \text{ M}^{-1}$. Because little DTNB remains at the end of the fast phase, the slow phase closely corresponds to the approach to equilibrium of the single reaction 5 with [Ac-Cys]_{initial} ≈ [Ac-Cys]₀ and [Cys-TNB]_{initial} ≈ [DTNB]₀. The ΔOD for this phase also corresponds to 1.0 TNB per starting DTNB, such that $k_{\text{obsd,slow}} \approx k_3[\text{Ac-Cys}]_0$ and $k_3 = 2.26 \pm 0.09 \text{ s}^{-1} \text{ M}^{-1}$. Thus, when DTNB concentration is in excess, almost all Ac-Cys molecules will be consumed by reaction 4 instead of reaction 5 since $k_1 = 60k_3$ and [DTNB] > [Ac-Cys-SS-TNB]. In this case, one expects single exponential behavior with $k_{\text{obsd}} \approx k_1[\text{DTNB}]_0$. The results agreed with expectations, giving $k_1 = 132 \pm 5 \text{ s}^{-1} \text{ M}^{-1}$, essentially identical with the value obtained in the biphasic experiment.

Previous studies of the pH dependence of k_{obsd} for the reaction of Ac-Cys with DTNB at high ionic strength gave an increase in k_{obsd} with increasing pH over the pH range 6–8 (Wenck & Schneider, 1971). Quantitative analysis of the dependence indicated that k_{obsd} results from nucleophilic attack of the thiolate form of Ac-Cys on the disulfide of DTNB. The thiol form of Ac-Cys does not react with DTNB.

In principle, the details of the reaction of Ac-Cys with DTNB may be complicated. An Ac-Cys molecule entering the electrostatic sphere of influence of DTNB is surrounded by water at all times and may undergo protonation or deprotonation during its trajectory through this sphere or even in a collision complex with DTNB. Equation 9 applies to the simple model where an Ac-Cys molecule remains protonated or deprotonated from the moment it enters the sphere to the

moment it reacts successfully or leaves the vicinity of the DTNB. Application of this equation to the data gives $Z_i Z_j = +4.0 \pm 0.8$, consistent with the values $Z_i = Z_{\text{DTNB}} = -2$ and $Z_j = A_{\text{Ac-Cys}}$ (reactive thiolate form) = Z_{base} (eq 2) = -2 expected when carboxyl charges and S⁻ are included in calculations of Z values. Thus, eq 9 appears to be quantitatively adequate for characterizing simple disulfide exchange reactions.

Kinetics of the Reaction between DTNB and STI: DTNB Concentration Dependence. In two-cysteine fragments, a variety of types of reaction steps may occur. These include bimolecular reaction of free cysteines with DTNB, intramolecular disulfide exchange between a free cysteine and a Cys-TNB on the same molecule to give a disulfide-bridged loop and free TNB, and intermolecular disulfide exchange involving two peptide molecules. Let k_A and k_B equal the bimolecular rate constants for reaction of DTNB with the peptide's two cysteines A and B, respectively. Let k_{ring} represent either of the ring-closure reactions (Cys_A attacking Cys_B-TNB or Cys_B attacking Cys_A-TNB) which in principle may differ in velocity. For an individual peptide molecule with DTNB concentration in excess, $k_A[\text{DTNB}]$, $k_B[\text{DTNB}]$, and k_{ring} are proportional to the probabilities for blocking to occur at Cys_A or Cys_B or for ring closure to occur in the singly blocked species.

Consider the case where $k_{\text{ring}} \gg k_A[\text{DTNB}]$ or $k_B[\text{DTNB}]$. In principle, one can work under these conditions at sufficiently low [DTNB] (and still lower [peptide] to maintain [DTNB] in excess) provided that the molarity of TNB produced is large enough to detect optically. Here, ring closure occurs almost instantly after the initial cysteine blocking. The overall reaction is kinetically equivalent to a single rate-limiting step yielding one ring and two TNB molecules (eq 10–12). Given excess DTNB and the possibility of DTNB reaction at either cysteine, each kinetic experiment would give a single exponential decay (eq 8) and $k_{\text{obsd}} = [\text{DTNB}]_0(k_A + k_B)$. If one bimolecular rate constant is much faster than the other ($k_A \gg k_B$), the term $k_A + k_B \approx k_A$ and $k_{\text{obsd}} = [\text{DTNB}]_0 k_A$.

At the opposite extreme obtained by working at very high [DTNB], a possible situation if all the DTNB is soluble and the blocking velocities are not too fast for stopped-flow time scales, $k_{\text{ring}} \ll k_A[\text{DTNB}]$ or $k_B[\text{DTNB}]$. Here, a singly blocked peptide will become doubly blocked before it has time to form the intramolecular ring. When k_A is distinctly different from k_B , the two independently reacting cysteines would give data appearing like the sum of two exponentials (eq 7) with $k_1 = k_{\text{obsd,fast}} = k_A[\text{DTNB}]_0$, $k_{\text{II}} = k_{\text{obsd,slow}} = k_B[\text{DTNB}]_0$, and equal amplitudes for both fast and slow phases (amp_I = 0.5).

Thus, a molecule with $k_A \gg k_B$ would exhibit the following behavior. At low [DTNB], kinetics will be single exponential with k_{obsd} proportional to [DTNB]. As [DTNB] increases, the point will be reached where $k_A[\text{DTNB}]$ is comparable in magnitude to k_{ring} . At this point, kinetic behavior will deviate from a single exponential as the two steps in the consecutive reaction become kinetically distinct. As [DTNB]₀ is increased, the initial blocking of the peptide will continue to increase in velocity, giving a k_{obsd} continuing to rise with [DTNB], but the line will curve since $k_{\text{obsd}} = (k_A + k_B)[\text{DTNB}]_0$ at low [DTNB] converts to $k_{\text{obsd,fast}} \approx k_A[\text{DTNB}]_0$. As $k_B[\text{DTNB}]$ increases in size relative to k_{ring} , $k_{\text{obsd,slow}}$ will approach the value $k_B[\text{DTNB}]_0$ and will show an increase as [DTNB] increases.

STI exhibits the qualitative features of the behavior described above (Figure 5B). At [DTNB] < 100 μM, single exponential behavior occurs with $k_{\text{obsd}} \propto [\text{DTNB}]$. The

Table I: Contributions of Cysteine Environments to Kinetics of Reaction with DTNB

species ^a	total charge ^b	local charge ^d			Z _i	
		2	1	0	cor ^e	uncor
Ac-Cys	-2			-2	-2.0 ± 0.4	
PEP	-7					-1.9 ± 0.2 ^c
293		-1	-1			
326		-2	-1			
STI	-5					≈0
145		-2	0			
136		-1	-1			
Cys-OEt	0			0		≈0
LYS	+3				+1.7 ± 0.3 ^c	
115		+1	+1			
127		0	0			

^a Based on sequences in Dayhoff (1978). ^b With one S⁻ and with homoserines not in lactone form. ^c The absolute value is an upper limit. ^d Charge includes neighbors within the indicated number of positions away from the cysteine. ^e Corrected for secondary salt effect.

transition from single exponential to multiple exponential behavior occurs from 100 to 400 μ M DTNB. $k_{\text{obsd}} = 0.5 \text{ s}^{-1}$ is the approximate value of the beginning of this transition, providing a rough estimate of $k_{\text{ring}} \approx 0.5 \text{ s}^{-1}$ (τ intramolecular exchange = 2 s) at pH 7.0, $\mu = 40 \text{ mM}$. At concentrations above 400 μ M, the data may be fit by the sum of two exponentials. At this point, $k_{\text{obsd,fast}}$ and $k_{\text{obsd,slow}}$ increase with [DTNB] and therefore include components of DTNB-blocking reactions. The apparent trend for a decreasing rise in $k_{\text{obsd,fast}}$ at high [DTNB] may be real and correspond to the expectations suggested above.

Although a detailed quantitative analysis of the complete DTNB concentration dependence is not yet possible, it is possible to equate $k_{\text{obsd}}/[\text{DTNB}]_0 = \text{rate-limiting initial blocking} = k_A + k_B$ in the ionic strength studies at 200 μ M DTNB (30-fold excess over total peptide SH concentration).

Background for Consideration of STI Kinetics: Ionic Strength Dependence. In proteins, charged groups on amino acids immediately adjacent to cysteine in the primary sequence may be positioned at greater distances from the sulfur atom than the 5 Å possible in Ac-Cys. Inspection of CPK space-filling models reveals that the maximum separation may extend to 10–13 Å for the short aspartate and long arginine side chains, respectively. The maximum extended distance for the side chains of residues located two or more positions from the cysteine position in the sequence may be calculated by adding 3.5 Å per amino acid to the above values. Of course, charged groups need not be located at this maximum distance. For nearest-neighboring residues, a minimum sulfur/charged group separation of 4 Å is possible.

To investigate whether neighboring residues contribute significantly to a cysteine's participation in disulfide exchange, it would be advantageous to study a pure polypeptide with a single cysteine. Furthermore, the sign of the charge of the neighboring residues should be different from the sign of the net charge of the total peptide in order to differentiate local environmental effects from general attraction or repulsion of DTNB by the peptide itself. Finally, the peptide should exist in a soluble random-coil monomeric state so that ionic strength variations reflect changes in reactions of exposed cysteines rather than changes in sulfhydryl accessibility due to salt-

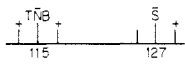

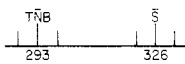
dependent changes in protein structure.

The two-cysteine fragment STI possesses most of these desired features. Circular dichroism studies of the derivatives with cysteines carboxymethylated or paired in an intramolecular disulfide indicate that these derivatives are random coils and monomeric at pH 7 and [peptide] = 13 μ M (Toniolo et al., 1978). It is reasonable to expect that STI with reduced SH groups, studied here at [peptide] = 3.5 μ M, will be structureless also. As seen in Table I, STI has two cysteines located at positions 136 and 145. As will be discussed below, the data suggest that DTNB reacts more quickly with Cys-145 than with Cys-136 such that the desired feature of single cysteine kinetics is met in practice. The overall charge of STI with Cys-145 in the thiolate form is -5, a negative value, whereas the local environment of first neighbors is positive. Second, third, and fourth nearest neighbors are negative.

The Debye-Hückel relationship was derived for situations where the charges of a polyion like Mg^{2+} are centrally located. The reactive group lies at the center of its own electrostatic sphere of influence which decreases in size as the ionic strength increases. The polyion region near Cys-145 is more complicated since charges are distributed in space. At low ionic strengths where electrostatic spheres of influence are large, many charged groups might contribute to the electric field experienced by an incoming DTNB molecule, including the negative aspartate-143 and aspartate-147 side chains two residues removed from cysteine-145. At higher ionic strengths, the effects on DTNB may be limited to electric fields associated with the thiolate anion itself plus only the lysine cation on the closest neighbor 146.

For a net negative thiolate region, the k_1 for reaction with DTNB will increase as μ increases both because the primary salt effect decreases repulsion between the molecules and because the secondary salt effect lowers the sulfhydryl pK, increasing f_{S^-} . In contrast, for a net positive thiolate region, the primary and secondary salt effects act in concert to decrease k as μ increases. For a net neutral region, a primary salt effect is not expected. The secondary salt effect is more complicated. For $\mu < 20 \text{ mM}$, the secondary salt effect in the zwitterion glycylglycine leads to the pK changes discussed earlier. From $\mu = 20$ –500 mM (the highest μ studied), the

Table II: Relative Rates of Intramolecular Exchange in DTNB Derivatives of Two-Cysteine Fragments

species	contributing effect			relative $k_{\text{intramolecular}}$	
	distance between Cys	1° salt effect	f_{S^-}	predicted	obsd (s^{-1})
LYS 	close	none	higher	fastest	>5.5
STI 	close	none	lower	intermediate	≈0.5
PEP 	distant	repulsion	lower	slowest	≈0.1 ^a

^a Assuming intermolecular exchange is negligible.

pKs of the amino and carboxyl groups are almost independent of ionic strength, confined to a narrow pK range of 0.025 unit (Neuberger, 1937). A complete fit to all of the carboxyl titration data, for example, required the following equation:

$$\text{pK} = \text{pK}^0 + \text{I} + \text{II}$$

$$\text{pK} = \text{pK}^0 + (Z_{\text{acid}}^2 - Z_{\text{base}}^2) \frac{A\mu^{1/2}}{1 + Br_1\mu^{1/2}} + \beta\mu \quad (19)$$

where Br_1 was arbitrarily set equal to 1.0 and the fitted value of β was 0.4. β is a function of the distance between the positive and negative groups. From $\mu = 20$ –500 mM, terms I and II are of opposite sign and similar magnitude, giving a small net secondary salt effect. The theoretical basis of term II was discussed in the original paper. Thus, at intermediate ionic strengths, it would be possible for a zwitterion thiolate region of dimensions similar to that of glycylglycine to exhibit little change in k due to the lack of a primary salt effect and the lack of a significant net secondary salt effect.

Ionic Strength Dependence of the Kinetics of Reaction of STI with DTNB. The ionic strength dependence of the kinetics of reaction of STI and DTNB is summarized in Figure 3. At $\mu > 20$ mM, it behaves like a net neutral zwitterion region as described above. In STI, only cysteine-145 plus its nearest neighbors comprise a net neutral region. Significant additional contributions from cysteine-136, neighbors beyond the immediately adjacent residues, or the overall peptide charge would lead to negative region behavior. Such contributions do occur at $\mu < 20$ mM ($\mu^{1/2} < 0.14 \text{ M}^{1/2}$), when electrostatic spheres of influence are large. The simplest explanation consistent with the STI data is the following model: (1) the charged groups on the amino acids immediately adjacent to a cysteine in the primary sequence are sufficiently close to contribute significantly to the effective net charge at the reactive thiolate region; (2) amino acids two or more positions from the cysteine do not contribute significantly to the kinetics at $\mu > 20$ mM but do contribute at lower ionic strengths; and (3) when the two thiolate regions (cysteines plus first nearest neighbors) of a two-cysteine peptide differ in charge by one or more units as in STI, the least negative region (Cys-145) will dominate the DTNB kinetics ($k_{145} + k_{136} \approx k_{145}$).

Reaction of LYS with DTNB and DTP. LYS was examined to determine the magnitude of the changes which may be achieved by converting from a cysteine with one positive neighbor (STI Cys-145) to a cysteine with two adjacent positive neighbors (LYS Cys-115). Since CD data have not been published for LYS, there is no direct evidence that this

peptide is monomeric and random coil in the conditions used here. Nevertheless, its low molecular weight (M 2860) probably precludes formation of a stable tertiary structure as a monomer, the low concentrations used here ($0.55 \mu\text{M}$ for μ -dependence studies) should minimize formation of aggregates, and the observation of $k_{\text{obsd}} \propto [\text{DTNB}]_0$ precludes contribution of DTNB-independent intermolecular disulfide exchange to k_{obsd} . Thus, the LYS data will be treated as corresponding to exposed cysteines. Any burying of cysteines in LYS would have to mean that the intrinsic k values for LYS are an even greater order of magnitude faster relative to those of STI than will be suggested here.

Because LYS Cys-115 has two positive neighbors whereas Cys-127 has only one positive neighbor, the model predicts that Cys-115 will react more rapidly and dominate the observed kinetics at $[\text{DTNB}]_0$ low enough to ensure that $k_{\text{ring}} \gg k_{\text{A}}[\text{DTNB}]$ or $k_{\text{B}}[\text{DTNB}]$. Under all conditions, the LYS data were single exponential in character with the fastest measured k_{obsd} equal to 5.53 s^{-1} . The single exponential behavior and $k_{\text{obsd}} \propto [\text{DTNB}]_0$ therefore suggest that $k_{\text{ring}} > 5.53 \text{ s}^{-1}$ in LYS. This is an order of magnitude faster than the estimate for k_{ring} in STI but still is consistent with the nearest-neighbor model. Table II lists the predicted products of initial DTNB blocking in LYS and STI. For both products, the cysteine and disulfide regions on the same molecule are approximately the same number of residues apart. Thus, the frequency of random intramolecular cysteine/disulfide collisions in the absence of electrostatic factors would be about the same in both types of molecules. A primary salt effect is not expected, since either the thiolate region (Cys-127 in LYS) or the disulfide region (Cys-TNB-145 in STI) is net neutral. However, a lower pK and greater f_{S^-} are expected for the thiolate region in singly blocked LYS (thiolate-127) than in singly blocked STI (thiolate-136). This would give k_{ring} in LYS $> k_{\text{ring}}$ in STI.

The ionic strength dependence of the kinetics of reaction of LYS with DTNB is included in Figure 3. An empirical estimate of $f_{\text{S}^-}/f_{\text{S}^0}$ may be obtained by reacting LYS with a neutral disulfide. A neutral disulfide will neither be attracted nor be repelled by the thiolate region but will reflect ionic strength dependent changes in the fraction of cysteines in the reactive thiolate form. DTP is a possible candidate. The pK for the second nitrogen deprotonation equals 2.45 (Brocklehurst & Little, 1973) such that the neutral form instead of the positive form of DTP predominates at pH 7.0. The result of using DTP to obtain an empirical function for $f_{\text{S}^-}/f_{\text{S}^0}$ in eq 9 is a value of $Z_i = 1.7 \pm 0.3$ corrected for the secondary salt effect.

Table III: Comparison of Absolute Values of Bimolecular Rate Constants

	$k_{\text{bimolecular}}$		
	PEP 293 ^a	STI 145 ^b	LYS 115 ^c
$\mu = 0$	155	1260	856000
$\mu = 20$ mM	367	3350	132000
$\mu = \infty$	8200	3980	1190

^a The k values for PEP have been divided by 2. No charged Cys neighbors present. ^b One positive charged Cys neighbor. ^c Two positive charged Cys neighbors.

A possible objection to this approach is that the relative contributions of cysteines-115 and -127 to reaction with DTNB may differ from their relative contributions to reaction with DTP. However, Cys-115 should dominate DTP kinetics since its pK should be lower than the Cys-127 pK and give greater f_S . Moreover, since cysteine-127 is a zwitterion region, it is expected to exhibit little salt-dependent change in f_S from $\mu = 20$ –500 mM as discussed above, such that even if it contributes to the absolute value of $k_{\text{obsd}} = (k_{A,DTP} + k_{B,DTP}) \cdot [DTP]_0$, changes in k_{obsd} should be caused by changes at cysteine-115.

It should be noted that DTP^+ , the minor species at pH 7, sometimes contributes to kinetic results by reacting with protonated thiol groups in an electrophilic substitution reaction (Brocklehurst & Little, 1972). For DTP^+ reactions, secondary salt effects on LYS sulfhydryl pK s will have little consequence since the predominant SH form (reactive with DTP^+) would experience a small fractional change in concentration. Secondary salt effects on DTP would raise the pK and increase the minor DTP^+ form at higher salt concentration, thereby increasing the DTP^+ kinetics. The primary salt effect also would increase kinetics by reducing repulsion between DTP^+ and the 115 thiol region (+2 for the thiol form) or the 127 region (+1 for the thiol form). Thus, DTP^+ electrophilic contributions would give an increasing k at higher ionic strengths, opposing the DTP nucleophilic contributions which give a decreasing k . The results in Figure 3 show a predominance of DTP (neutral form) nucleophilic reaction kinetics at pH 7 and provide a minimum estimate of the DTP rate-lowering results, a minimum estimate of the secondary salt effect in Cys-115/DTNB kinetics, and an upper limit to the absolute value of the Z_i . The upper limit of $+1.7 \pm 0.3$ therefore is consistent with the model's prediction of $Z_i \approx +1$.

The smooth shape of the LYS/DTNB curve contrasts with the STI data. The change from negative region behavior to zwitterion region behavior as μ increases was attributed above to the decreasing electrostatic sphere of influence associated with negative groups located at a large distance from the cysteine, including the two amino acids two residues away. For LYS Cys-115, both residues two positions away are neutral such that long-range contributions would have to come from residues further along the sequence. As such, a smoother shape might be expected for LYS as compared with STI.

Table III compares the absolute rate constants for DTNB reaction with LYS and STI. At zero ionic strength, there is a 680-fold difference in LYS and STI rate constants, which may include contributions from the overall peptide charge. The relative rate constants at infinite ionic strength, given by eq 9 for LYS and the apparent asymptote approached by STI data in Figure 3, differ by a factor of 3. Given the rough nature of such estimations, the calculations are consistent with the expectation that Coulombic influences will vanish at infinite ionic strengths and all peptide cysteines will behave identically.

At $\mu = 20$ mM, where effects are indicative of the neighbors immediately adjacent to the cysteines, the rate constants differ by a factor of 39. The ΔG^* for these rate constants may be represented as follows where the STI 145–147 thiolate region is net neutral, the LYS 114–116 thiolate region is net +1, and the DTNB disulfide region is -2 in charge:

$$\Delta G^*(\text{DTNB/LYS}) =$$

$$\Delta G^*_{\text{DTNB disulfide stability}} + \Delta G^*_{\text{electrostatic}} (-2/+1) \quad (20)$$

$$\Delta G^*(\text{DTNB/STI}) =$$

$$\Delta G^*_{\text{DTNB disulfide stability}} + \Delta G^*_{\text{electrostatic}} (-2/0) \quad (21)$$

$$\Delta(\Delta G^*) = \Delta(\Delta G^*_{\text{electrostatic}}) = \text{two charge-pair interactions} \\ = -RT \ln (k_{\text{LYS}}/k_{\text{STI}}) = -2.2 \text{ kcal/mol} \quad (22)$$

where $R = 0.002 \text{ kcal mol}^{-1} \text{ K}^{-1}$ and $T = 296 \text{ K}$. These equations represent the disulfide exchange reaction as the sum of electrostatic factors (both primary and secondary salt effects) and the requirement for breaking the disulfide bond in DTNB, including steric effects. The 39-fold difference in rate constants then corresponds to the difference in electrostatic factors. The results give 1.1 kcal/mol per ion pair interaction, a reasonable order of magnitude for an ion pair in aqueous solution. If DTNB were replaced by a peptidelike molecule, such as a disulfide linking two aspartate(–)-cysteine sequences, the absolute values of rate constants would be lower since ΔG^* (DTNB disulfide stability) will be less than ΔG^* (cystine disulfide stability), but the relative rates of reaction with LYS and STI still would be represented by $\Delta(\Delta G^*_{\text{electrostatic}})$. The possible COO^- to S distance in aspartate–cysteine (4–10 Å) is comparable to that in TNB (5–6 Å). Furthermore, the lysine and thiolate ions in STI lysine-145(+)-cysteine-146(–) give a net neutral region. Thus, it is reasonable to predict that the $\Delta(\Delta G^*_{\text{electrostatic}})$ in peptide–cysteine/peptide–disulfide interactions will be comparable to $\Delta(\Delta G^*_{\text{electrostatic}})$ in the DTNB data. The maximum range of local environmental electrostatic effects would correspond to reaction of a thiolate region bordered by aspartates (–3) with a disulfide region (–4) having four nearest-neighbor aspartates (two per cysteine) vs. reaction with a disulfide region bordered by four lysines (net +4). The –3/–4 vs. –3/+4 difference corresponds to 24 charge-pair interactions. For $\Delta G/\text{charge pair} = 1.1 \text{ kcal/mol}$, this would give an achievable (2×10^{19})-fold range in rate constants at $\mu = 20 \text{ mM}$. A more conservative estimate of 0.34 kcal/mol per charge pair would give a (1×10^6)-fold range.

Supplementary Information from Reaction of DTNB with Cys-OEt and PEP. The amine and sulfur groups in Cys-OEt are as close together as the carboxyl and sulfur groups in Ac-Cys. At $\mu = 60$ –100 mM, four separate pK s have been determined in Cys-OEt (Benesch & Benesch, 1955) for the amine titration in the S^- and SH molecules and the sulfhydryl titration in the NH_3^+ and NH_2 molecules. With these pK s, iterative calculations reveal that 11.6% of the molecules at pH 7 exist as the $^+\text{H}_3\text{N}-\text{R}-\text{S}^-$ form and 0.4% as the $\text{H}_2\text{N}-\text{R}-\text{S}^-$ form. Thus, 96% of the reactive thiolate molecules are in the zwitterion net neutral form at the above ionic strength. The rate constant for the reaction of Cys-OEt with DTNB is essentially independent of ionic strength, as seen in Figure 3. The lack of a μ dependence in k in the vicinity of $\mu = 80 \text{ mM}$ is consistent with the above discussions of the expected behavior for zwitterion thiolate regions.

The [DTNB] dependence of PEP kinetics in Figure 5A exhibits a single rate-limiting blocking step at low [DTNB]₀ and multiple steps at higher [DTNB]₀ as in STI. DTNB-independent processes, either inter- or intramolecular, begin to appear at a time scale corresponding to $k = 0.1 \text{ s}^{-1}$ ($\tau =$

10 s). The possibility of intermolecular exchange processes between aggregated peptide molecules should not be ruled out since PEP begins to precipitate at pHs below 6.5, only slightly lower than the pH 7.0 used in these experiments. If $k = 0.1 \text{ s}^{-1}$ were reflecting intramolecular ring formation, k_{ring} in PEP would be less than k_{ring} in STI. As seen in Table II, this rank order would be consistent with the nearest-neighbor model. Singly blocked STI and PEP would exhibit similar secondary salt effects given a thiolate region of -1 charge, but the larger thiolate/disulfide separation in the sequence of PEP and the electrostatic repulsion between those regions in PEP would lower collision frequencies relative to those in STI.

Table I indicates that cysteines-293 and -326 both have neutral neighbors in immediately adjacent positions. The second nearest neighbors of cysteine-293 also are neutral, whereas an additional negative charge occurs at position 324. Thus, at $\mu \geq 20 \text{ mM}$, the nearest-neighbor model predicts that both 293 and 326 will contribute equally to kinetics, with $k_{\text{obsd}} = (k_{293} + k_{326})[\text{DTNB}]_0 = 2k_{293}[\text{DTNB}]_0$ and $Z_i \approx -1.0$, the charge on the thiolate sulfur. From 0 M to 20 mM, a Z_i of greater absolute value may be exhibited due to contributions from the overall peptide charge (-7 or -8) or as a result of aspartate-324(−) acting on Cys-326.

The ionic strength dependence of PEP kinetics presented in Figure 3 exhibits characteristics which are consistent with the above expectations. At low μ , there may be a strongly negative behavior which decreases in magnitude above $\mu = 20 \text{ mM}$. The overall fit to the data without correction for the secondary salt effect gives $Z_i = -1.9 \pm 0.2$. Correction for the secondary salt effect which acts in concert with the primary effect would give a true Z_i of smaller absolute magnitude, closer to the expected $Z_i = -1.0$. PEP's behavior strongly indicates that the overall peptide charge does not play a significant role at $\mu \geq 20 \text{ mM}$. PEP has only one positive group but seven–eight negative groups, such that the overall peptide would appear uniquely and strongly negative to a DTNB molecule approaching the peptide if the overall peptide charge influenced kinetics.

The absolute values of PEP rate constants are included in Table III. The following discussion used $k_{293} = k_{\text{obsd}}/2 - [\text{DTNB}]_0$, based on the assumption that $k_{293} \approx k_{326}$ at $\mu \geq 20 \text{ mM}$. k° for PEP approaches the value observed in STI. At $\mu = 20 \text{ mM}$, k_{STI} and k_{PEP} differ by a factor of 9.1, corresponding to a difference of two ion pair interactions and 0.65 kcal/mol per ion pair. This is less than the value obtained by comparing LYS and STI (1.1 kcal/mol) but greater than the value of 0.34 kcal/mol used to obtain the conservative estimate of an achievable (1×10^6)-fold range of values for disulfide exchange rate constants.

Strategies for Directing Disulfide Pairing in Proteins. In conclusion, these studies suggest the following points relevant to strategies for directing disulfide pairing in proteins. (1) Reactions should be performed at pH 7, well below cysteine pKs, to enhance the percent changes in f_S^- due to secondary salt effects. (2) The ionic strength should equal 20 mM to restrict ionic influences to charged residues immediately adjacent to cysteines in the primary sequence. (3) Under these conditions, the local electrostatic environments give an achievable range of rate constants estimated to be 10^6 -fold or greater, large enough to be employed to significant advantage in strategies for directing disulfide pairing in synthetic polypeptides.

Acknowledgments

The authors appreciate the technical assistance of Robert Spengler in performing amino acid analyses.

References

- Archarya, A. S., & Taniuchi, H. (1976) *J. Biol. Chem.* 251, 6934.
- Bates, R. G., & Bower, V. E. (1956) *J. Res. Natl. Bur. Stand., Sect. A* 57, 153.
- Benesch, R. E., & Benesch, R. (1955) *J. Am. Chem. Soc.* 77, 5877.
- Berger, R. L., & Stoddart, L. C. (1965) *Rev. Sci. Instrum.* 36, 78.
- Bieth, J., & Frechin, J. C. (1974) in *Proteinase Inhibitors* (Fritz, H., Tschesche, H., Greene, L. J., & Truscheit, E., Eds.) pp 291–304, Springer-Verlag, New York.
- Bodner, B. L., Jackman, L. M., & Morgan, R. S. (1980) *Biochem. Biophys. Res. Commun.* 94, 807.
- Brocklehurst, K., & Little, G. (1972) *Biochem. J.* 128, 417.
- Brocklehurst, K., & Little, G. (1973) *Biochem. J.* 133, 67.
- Chang, C. C., Yang, C. C., Nakai, K., & Hayashi, K. (1971) *Biochim. Biophys. Acta* 251, 344.
- Chen, K. C. S., Tao, N., & Tang, J. (1975) *J. Biol. Chem.* 250, 5068.
- Creighton, T. E. (1975) *J. Mol. Biol.* 96, 767.
- Datta, S. P., & Grzybowski, A. K. (1966) *J. Chem. Soc. B*, 136.
- Davis, D. G., Gisin, B. G., & Tosteson, D. C. (1976) *Biochemistry* 15, 769.
- Dayhoff, M. O. (1978) in *Atlas of Protein Sequence and Structure*, Vol. 5, Supplement 3, National Biomedical Research Foundation, Silver Spring, MD.
- Grassetti, D. R., & Murray, J. F., Jr. (1967) *Arch. Biochem. Biophys.* 119, 41.
- Hardy, P. M., Ridge, B., Rydon, H. N., & Serrao, F. O. S. P. (1971) *J. Chem. Soc. C*, 1722.
- Hass, G. M., Ako, H., Grahm, D. T., & Neurath, H. (1976) *Biochemistry* 15, 93.
- Hird, F. J. R. (1962) *Biochem. J.* 85, 320.
- Kauzmann, W. (1959) in *Sulfur in Proteins* (Benesch, R., et al., Eds.) p 93, Academic Press, New York.
- Koide, T., & Ikenaka, T. (1973) *Eur. J. Biochem.* 32, 401.
- LaMer, V. K. (1932) *Chem. Rev.* 10, 179.
- Lee, M. L., & Safille, A. (1976) *J. Chromatogr.* 116, 462.
- Mihalyi, E. (1969) *J. Chem. Eng. Data* 13, 179.
- Morgan, R. S., Tatsch, C. E., Gushard, R. H., McAdon, J. M., & Warme, P. K. (1978) *Int. J. Pept. Protein Res.* 11, 209.
- Neuberger, A. (1937) *Proc. R. Soc. London, Ser. A* 100, 68.
- Nolte, H. J., Rosenberry, T. L., & Neumann, E. (1980) *Biochemistry* 19, 3705.
- Owen, B. B. (1934) *J. Am. Chem. Soc.* 56, 1695.
- Paul, C., Kirschner, K., & Haenisch, G. (1980) *Anal. Biochem.* 101, 442.
- Perutz, M. F. (1976) *Nature (London)* 262, 449.
- Riddles, P. W., Blakeley, R. L., & Zerner, B. (1979) *Anal. Biochem.* 94, 75.
- Ruhlmann, A., Kukla, D., Schwager, P., Bartels, K., & Humber, R. (1973) *J. Mol. Biol.* 77, 417.
- Stevens, F. C., Wuerz, S., & Krahn, J. (1973) in *Proteinase Inhibitors* (Fritz, H., Tschesche, H., Greene, L. J., & Truscheit, E., Eds.) p 394, Springer-Verlag, New York.
- Szajewski, R. P., & Whitesides, G. M. (1980) *J. Am. Chem. Soc.* 102, 2011.

Tan, N. H., & Kaiser, E. T. (1977) *Biochemistry* 16, 1531.
 Toniolo, C., Bonora, G. M., Vita, C., & Fontana, A. (1978) *Biochim. Biophys. Acta* 532, 327.
 Weber, U., & Hartter, P. (1974) *Hoppe-Seyler's Z. Physiol.*

Chem. 355, 200.
 Weber, U., & Schmid, H. (1976) *Hoppe-Seyler's Z. Physiol. Chem.* 357, 1359.
 Wenck, H., & Schneider, F. (1971) *Experientia* 27, 20.

Conformational Differences between High Clotting Human α -Thrombin and Nonclotting γ -Thrombin[†]

German B. Villanueva

ABSTRACT: The conformations of human α -thrombin and γ -thrombin have been compared by circular dichroism, solvent perturbation difference spectroscopy, and chemical modification. Circular dichroism studies indicate that proteolytic conversion of α -thrombin to γ -thrombin is accompanied by considerable conformational changes which include a decrease in α -helical content from 5-7% to 0-1%. Solvent perturbation at pH 6.0 obtained with 20% ethylene glycol, 20% glycerol, and 20% dimethyl sulfoxide indicates an apparent exposure of 3.5 ± 0.2 tryptophan and 7.8 ± 0.1 tyrosine residues in α -thrombin and 4.6 ± 0.2 tryptophan and 9.2 ± 0.3 tyrosine residues in γ -thrombin. This increased exposure is substan-

tiated by the greater reactivity of tryptophan residues in γ -thrombin toward dimethyl(2-hydroxy-5-nitrobenzyl)sulfonium bromide. It suggests that γ -thrombin is a less compact molecule than the parent α -thrombin. Solvent perturbation studies of α -thrombin and γ -thrombin inhibited by phenylmethanesulfonyl fluoride showed that 0.3 ± 0.4 tryptophan and 0.9 ± 0.3 tyrosine residues in α -thrombin and 0.6 ± 0.3 tryptophan and 1.3 ± 0.4 tyrosine residues in γ -thrombin were blocked by the inhibitor. These subtle differences in the extent of blocking of tyrosine and tryptophan suggest a tighter conformation in the catalytic site of γ -thrombin compared to that of α -thrombin.

It is known that multiple forms of thrombin with vastly differing specific activities toward protein and synthetic substrates can be isolated from activation mixtures of crude prothrombin (Mann et al., 1972; Seegers et al., 1968; Rosenberg & Waugh, 1970). Human α -thrombin, the form that is responsible for the clotting of blood, is a molecule composed of two polypeptide chains linked by a single disulfide bond (Thompson et al., 1977). This form of thrombin can be converted by autolysis or limited proteolysis to β -thrombin and subsequently to γ -thrombin. γ -Thrombin is characterized by a drastically reduced ability to clot fibrinogen, but its activity toward synthetic substrates and its ability to bind to anti-thrombin III are not significantly changed (Chang et al., 1979). In addition, γ -thrombin has retained its ability to activate factor XIII (Lorand & Credo, 1977) but has reduced ability to stimulate platelets (Charo et al., 1977).

Although the physiological significance of this form of thrombin is not known, γ -thrombin is an interesting model to study the active conformation of thrombin because proteolytic conversion of α -thrombin to γ -thrombin results in cleavage of the B chain at two places. On the basis of sequence homology with pancreatic proteases, this fragmentation separates the functional residues which are expected to participate in the charge relay system (His-57, Ser-195, and Asp-102). γ -Thrombin, however, retains these fragments through non-covalent association since complete separation of the B-chain fragments could only be shown when subjected to dissociating conditions, i.e., reduction, urea, and NaDodSO₄¹ (Lundblad et al., 1979; Fenton et al., 1979).

The observations that the kinetic parameters (measured by proflavin displacement) of α -thrombin and γ -thrombin show no significant differences and have essentially identical behavior with ester substrate (Chang et al., 1979) have led to

the suggestion that the active site and neighboring regions are unchanged by the α - to γ -thrombin conversion. Hence, it is believed that the loss of clotting activity of γ -thrombin during proteolysis must be related to as yet unexplained structural changes which are remote from the active site. Although reports have implicated conformational differences between these two forms because of different stabilities under denaturing conditions (Bauer et al., 1980), there is no direct experimental evidence, and the nature and extent of these differences are largely unknown.

In the present study, we have used solvent perturbation difference spectroscopy, circular dichroism, and chemical modification to investigate the conformational aspects of α -thrombin and γ -thrombin. The data presented here provide the first direct experimental proof of conformational differences between the two forms of thrombin in their native states.

Materials and Methods

Materials. Highly purified α -thrombin and γ -thrombin were generous gifts of Dr. John Fenton II, New York State Department of Health, Albany, NY. The enzyme purity (NaDodSO₄-gel electrophoresis), specific activities (clotting and esterase), and active-site concentration (NPGB titration) were done in Albany and checked in our laboratory. Two α -thrombin preparations were used with the following enzymatic properties: 3153 and 3005 (NIH) clotting units/mg; 96.7% and 93.9% active by NPGB titration; 99.5% α , 0.5% β , 0.0% γ and 95.5% α , 0.6% β , 3.9% γ . Two γ -thrombin preparations were used with the following enzymatic properties: 0.74 and 0.31 (NIH) clotting units/mg; 65.1% and

[†] From the Department of Biochemistry, New York Medical College, Valhalla, New York 10595. Received March 11, 1981. This investigation was supported by National Institutes of Health Grant HL 23265.

¹ Abbreviations used: Mes, 2-(N-morpholino)ethanesulfonic acid; NPGB, *p*-nitrophenyl *p*'-guanidinobenzoate; PMSF, phenylmethanesulfonyl fluoride; PMS- α -thrombin, phenylmethanesulfonyl- α -thrombin; PMS- γ -thrombin, phenylmethanesulfonyl- γ -thrombin; tosyl-Lys-CH₂Cl, 1-chloro-3-tosylamido-7-amino-2-heptanone hydrochloride; Tos-Arg-OMe, tosyl-L-arginine methyl ester; NaDodSO₄, sodium dodecyl sulfate.